Table 1. Main IR frequencies [cm^{-1}] and protonNMR chemical shifts (δ [ppm]) of *N*-methacryloyl-L-histidine

	Assignments
IR	1709 (*w*) C=O stretch of COOH group; 1656 (*s*) Amide I; 1620 (*sh*) C=C; 1600 (*vs*) Imidazole group; 1534 (*s*) Amide II; 1437 (*w*) $-CH_3$; 1393 (*vs*) C=O stretch of COO^- *w*: weak; *s*: strong; *sh*: shoulder; *vs*: very strong
^{1}H NMR	1.75 (s, 3H $CH_3C(=CH_2)H-$); 2.95–3.23 (m, 2H –CH2– Imidazole); 4.41–4.46 (q, H –NHC*H*(COOH)CH_2-); 5.31–5.52 (m, 2H $CH_2=C(CH_3)-$); 7.12 (s, 1H Imidazole, –C=C*H*N=); 8.44 (s, 1H Imidazole, –N=C*H*NH–)

potentiometric purity revealed that the imidazole nitrogen was protonated more than 92 wt%, while the carboxyl group was mostly in the ionized form. The expected structure was confirmed by the ^{1}H NMR and FT-IR spectroscopy. Table 1 summarizes the observed main infrared frequencies and the chemical shifts of the MHist.

Unlike the previously reported acrylate monomer, the *N*-acryloyl-L-histidine (Hist), the MHist showed the presence of a great amount of amphoteric molecular species [6]. The lower chemical shifts of the imidazole protons and the very strong band at 1600 cm^{-1} are indicative of the prevailing zwitterionic molecules [19]. This is also supported by the greater basicity constant.

Polymers

The *N*-methacryloyl-L-histidine, MHist, was used as the starting pH-sensitive monomer to synthesize free and cross-linked polymers together with the thermoresponsive *N*-isopropylacrylamide, NIPAAm, by a radical polymerization [4–6]. Unlike the poly(*N*-methacryloyl-L-histidine), the polyMHist, that was obtained in ethanol and using the AIBN initiator, the three copolymers with NIPAAm (co-3, co-2, and co-1), along with the three hydrogels (MH2, CMH2, and CMH10), were obtained in water solution by the use of the APS initiator [19–26]. While the free polymers remained in solution during the polymerization process, the cross-linked compounds gelified within 4 hrs. Compared to the acrylate analogue [6, 19], the polymerization of the methacrylate MHist to the corresponding

Table 2. Results of molecular characterization of polyMHist homopolymer and copolymers by SEC-MALS

Sample	MHist content [weight%]	dn/dc [ml/g]	M_p [kg/mol]	M_w [kg/mol]	M_w/M_n
PolyMHist	96.5	0.190	81.4	83.2	3.2
co-1	9.1	0.175	481.3	–	–
co-2	17.9	0.177	792.2	831.6	2.0
co-3	51.5	0.182	304.0	380.0	2.2

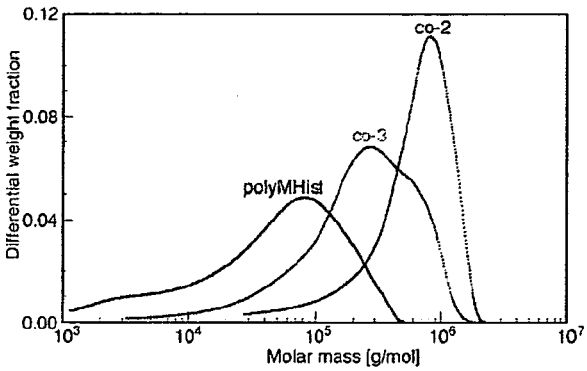

Figure 4. Comparison of the differential molar mass distribution of polyMHist homopolymer, co-2 and co-3 copolymers by SEC-MALS

homopolymer gave rise to a relatively lower number-average molecular weight, while the polydispersity index remained quite high, even after the dialysis process (Table 2).

This may be ascribed to the different solvent used in the polymerization procedure [25]. Figure 4 shows the comparison of the differential molar mass distribution (DMM) of the polyMHist homopolymer and the two copolymers (co-2 and co-3) bz SEC-MALS.

Unfortunately, the chromatographic elution of the copolymers depends on the NIPAAm content. In particular, Figure 4 does not report the DMM of co-1 copolymer because the chromatogram presents a long tail in consequence of a very high NIPAAm content (about 90%). Consequently, for the co-1 copolymer Table 2 reports only the peak molar mass M_p. It is important to note that the molar mass values from MALS are absolute and do not depend on an eventual non-steric chromatographic elution. As a result the M_w and M_p molar mass values are substantially correct, while the polydispersity index M_w/M_n (see Table 2) and in general the DMM shape (see Figure 4) are only approximate.

Table 3. Molar composition of vinyl polymers containing L-histidine residues

Compd	MHist purity, [mol%]	
	Potentiometry	Proton NMR
PolyMHist	96.5	100.0
co-3	35.0	36.5
co-2	10.0	8.2
co-1	4.9	3.5

The copolymers with NIPAAm produced higher molecular weight compounds that in general increased with the NIPAAm content. This led also to a greater viscosity in a wide range of pH (see the protonation section). However, in all cases the ^{1}H NMR spectra showed that the chemical shifts of the vinyl double bond (5.31–5.52 ppm) completely disappeared, and the broad lines were consistent with the presence of a slowly tumbling macromolecular species in D_2O solution. The FT-IR spectra confirmed the total conversion of the monomers into the corresponding polymers. The band intensity at 1599 cm^{-1} present in the polyMHist decreased as the NIPAAm unit increased in the copolymers. In the meantime, the new band of the NIPAAm Amide I increased and slightly shifted to greater wavenumbers, in the same way as happened for the 1459 cm^{-1} band of the isopropyl group [31, 32].

Based on the NMR and potentiometric results, the relative comonomer MHist/NIPAAm incorporation level reflected the comonomer feed ratio. Table 3 shows that the amount [mol%] of titrated MHist in the polymers is in agreement with that evaluated by the proton signals of the methyl groups.

These results suggest a presumably total conversion of the monomers into the corresponding polymers, being the reaction of radical type. A random distribution of MHist units in copolymers with NIPAAm may be expected because the basicity constants and the *n* values showed a decreasing trend (see protonation section). When both the monomers had a close structure, a random distribution of charged units was observed in the copolymer. This reflects lower electrostatic effects due to a lower content of charged groups. [25, 30, 32]. Moreover, the hydrogels, were obtained at the fixed amount of cross-linking agent (EBA, 2 and 10 mol%) and with a NIPAAm/MHist molar ratio of 0 and 12, in order to have, respectively, a greater content of pH- or temperature-responsive comonomer content. After the polymerization procedure, the samples were slowly dried at r.t. for a week and then under vacuum. As expected, the acid/base potentiometric titrations of the gel MH2 revealed that the imidazole nitrogen content of

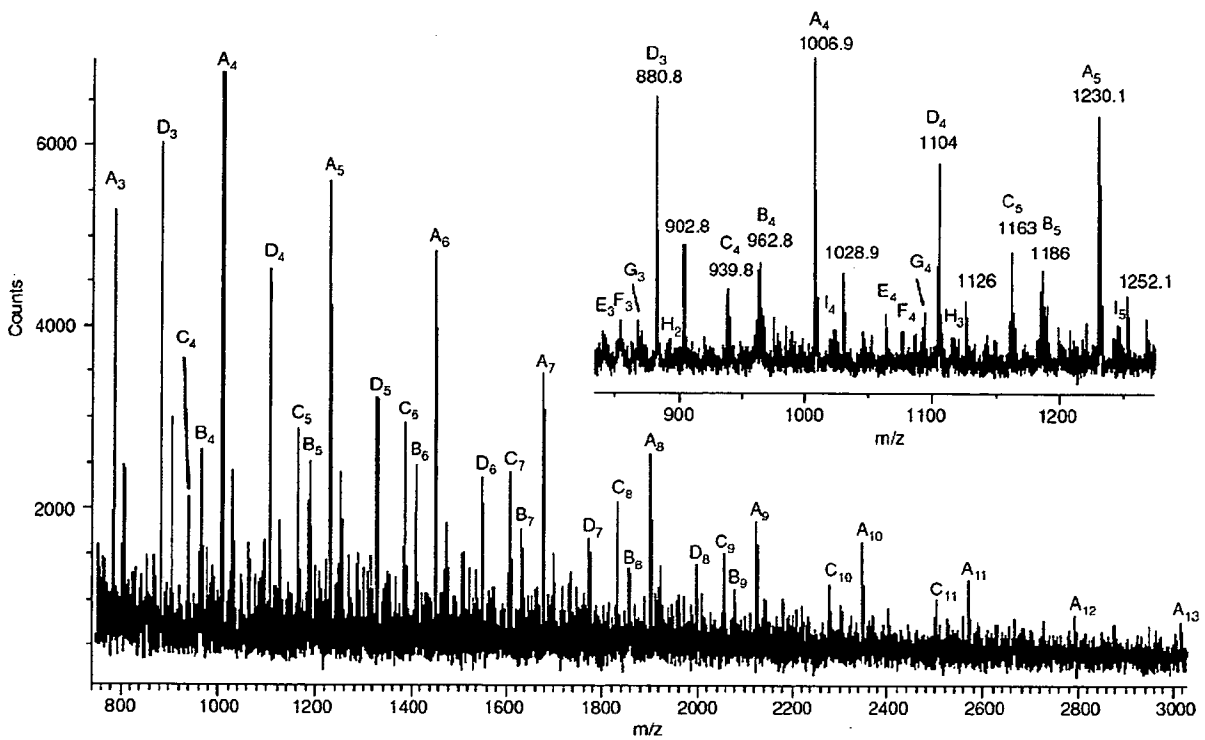

Figure 5. Positive ions MALDI-TOF mass spectrum of the polyMHist sample

Table 4. Structural assignments of peaks displayed in the MALDI-TOF mass spectrum of the polyMHist

Structures[a]	$[MH]^+$ (n)[b]	$[M+Na]^+$ (n)[b]
A= 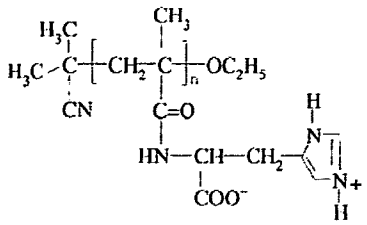	783.7 (3) 1006.9 (4) 1230.1 (5) 1453.3 (6) 1676.5 (7) 1899.7 (8) 2122.9 (9) 2346.1 (10) 2569.3 (11) 2792.5 (12) 3015.7 (13)	805.7 (3) 1028.9 (4) 1252.1 (5) 1475.3 (6) 1698.5 (7) 1921.7 (8) 2144.9 (9) 2368.1 (10) 2591.3 (11) 2814.5 (12) 3037.7 (13)
B= 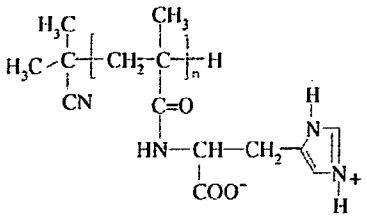	962.8 (4) 1186.0 (5) 1409.2 (6) 1632.4 (7) 1855.6 (8) 2078.8 (9) 2302.0 (10) 2525.2 (11) 2748.4 (12) 2971.6 (13)	984.8 (4) 1208.0 (5) 1431.2 (6) 1654.4 (7) 1877.6 (8) 2100.8 (9) 2324.0 (10) 2547.2 (11)
C= 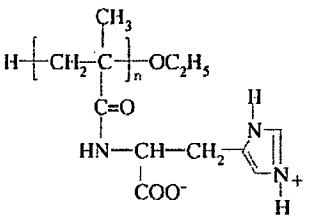	939.8 (4) 1163.0 (5) 1386.2 (6) 1609.4 (7) 1832.6 (8) 2055.8 (9) 2279.0 (10) 2502.2 (11) 2725.4 (12) 2948.6 (13)	961.8 (4) 1185.0 (5) 1408.2 (6) 1631.4 (7) 1854.6 (8) 2077.8 (9) 2301.0 (10) 2524.2 (11) 2747.4 (12) 2970.6 (13)
D= 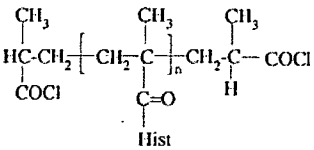	880.8 (3) 1104.0 (4) 1327.2 (5) 1550.4 (6) 1773.6 (7) 1996.8 (8)	902.8 (3) 1126.0 (4)
E= 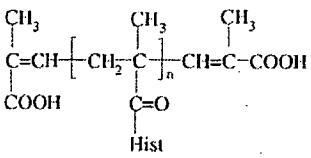	840.6 (3) 1063.8 (4)	
F= 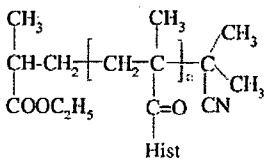	853.6 (3) 1076.8 (4)	
G= 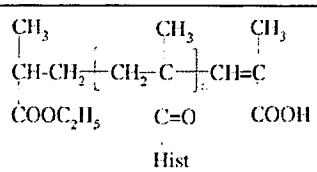	870.6 (3) 1093.8 (4)	

Table 4. Continued

Structures[a]	$[MH]^+$ (n)[b]	$[M+Na]^+$ (n)[b]
H= 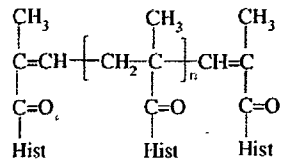	893.8 (2) 1117.0 (3)	
I= 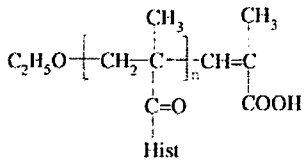	1023.8 (4) 1247.0 (5)	

a) Hist =

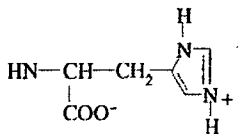

b) Values in parentheses are the repeating units

MHist was in agreement with the feed composition. The potentiometric curves showed large hysteresis loops [4] during the forward and backward titrations with NaOH and HCl solutions, respectively (Figure 3). This may be ascribed to the grinded state of the sample, considering that the MH2 gel particles were large and compact. The large size distribution of the material, along with its compactness, may slow down the equilibration for the protonation mechanism of the gel MH2, due to a hard deep diffusion of the hydrated H^+/OH^- ions into the interior of the gel particles. The potentiometric curves reached a faster equilibrium condition when a finely crushed sample of MH2 was titrated at the equilibration time of 1500 s and 3000 s for each titrant (H^+/OH^-) addition (Figure 3).

The MALDI-TOF mass spectrometry technique [33–35] has been used to characterize the chemical structures of the polyMHist oligomer components. Figure 5 reports a typical mass spectrum of the polyMHist, recorded in reflection mode, using HABA (0.1N in C_2H_5OH) as a matrix and the polymer dissolved in water. This spectrum exhibits a series of peaks from 750 up to 3000 Da corresponding to the protonated and sodiated ions of the polyMHist oligomers with a variety of the end groups, and they have been assigned (Table 4) to a specific oligomer structure. The identification of the structure and the end groups attached to the oligomers produced in the free-radical polymerization process is of utmost importance, since the end groups reveal the particular mechanisms that have been active in the polymerization process. The structures of the oligomers corresponding to the mass peak series A, and B in Figure 5, belonging to the expected oligomers terminated with isobutironitrile (IBN) groups at one end (Table 4), are due to the initial reaction of the radical initiator with the monomer MHist. The oligomers A are also terminated with an etoxyl group ($-OC_2H_5$) at the other end chain, indicating that a reaction between macroradicals and the ethanol used as solvent occurred. The oligomers B, besides the IBN groups, are terminated with H and are maybe generated by a H-extraction reaction, that occurs in a typical free-radical polymerization. The last two reactions led to the oligomers C which are terminated with –H and $-OC_2H_5$ species (Table 4). The intense peaks belonging to the mass series D were assigned to the unexpected oligomers terminated with methacryloyl chloride groups at both the ends. These are due to the metacryloyl chloride unit present as not detectable trace in the purified MHist used as monomer in the synthesis of the polyMHist sample. These peaks disappeared when the crude polyMHist sample was dissolved in ethanol to prepare the sample for the MALDI analysis, giving in this case intense mass peaks due to the corresponding oligomers with ethyl methacrylate end chains. Looking at the inset in Figure 5, we observe the

presence of weak mass peaks labelled as E, F, G and I (Table 4) corresponding to the oligomers that could be generated from oligomers terminated with metacryloyl chloride groups. Finally, the oligomers species indicated as H and I, as well as the species G, bearing unsaturated end groups (see Table 4) could be formed by the disproportionation reactions that occur during the conventional free radical polymerization.

3.2. Protonation study

Potentiometry, viscometry, and solution calorimetry were the main techniques used to study the protonation behaviour of the monomer, the polymer, the copolymers and the hydrogels at 25°C in aqueous 0.15M NaCl.

Basicity Constants and viscometry

The basicity constant values for the protonation of the basic imidazole nitrogen ($\log K_1$) and the carboxylate group ($\log K_2$) in the MHist and in the related polymer and copolymers are reported in Table 5. In the same table the basicity constants for the MH2 hydrogel is also reported.

The presence of the methyl groups in the main chain of the polymer structure strongly reduces the polyelectrolyte behaviour because of the increased hydrophobicity. The $\log K_1$ of the MHist (6.88) showed a greater value than that of the Hist (6.48) for inductive effects. On the other hand, the corresponding polymeric compound showed a quite similar $\log K$ value. The hydrogel MH2 showed greater $\log K$s and a lower n value; this trend, being similar to the previously studied acrylate hydrogels, may be attributed to the reduced conformational freedom because of the cross-linked network structure.

However, in all cases the $\log K$s follow the modified Henderson-Hasselbalch equation [36] showing a linear decreasing pattern on the degree of protonation α of the whole macromolecule. The experimental data, i.e. pH in relation to α, fitted very well the generalized Henderson-Hasselbalch equation (1):

$$pH = \log K_i^\circ + n \cdot \log[(1 - \alpha)/\alpha] \quad (1)$$

which has been checked experimentally for a number of polyelectrolytes [37, 38]. The linear relationship between pH and $\log[(1 - \alpha)/\alpha]$, over a wide range of α values, gives a straight line for all the compounds studied (Figure 6).

This led to exclude any transition region between the coil to compact structure, as occurred for other class of polyelectrolytes [37, 38]. The n value for the protonation of the imidazole nitrogen in the polyMHist and the corresponding copolymers, being related to the magnitude of the electrostatic interactions as well as being a measure of the hydrophilic influence [39], is always much lower than that reported for the acrylate analogue. Fur-

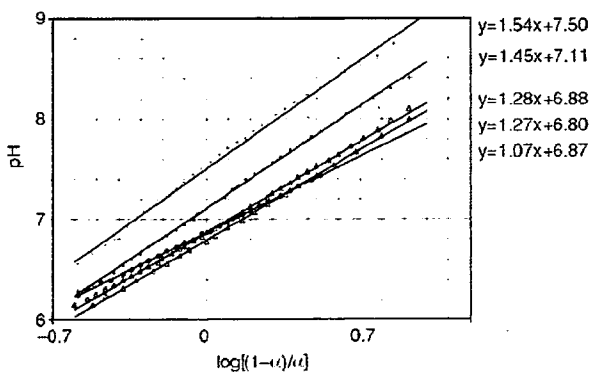

Figure 6. Typical Henderson-Hasselbalch plots of the MHist soluble compounds in 0.15M NaCl at 25°C

Table 5. Basicity constants of vinyl compounds containing L-histidine residues at 25°C in 0.15M NaCl

Compd	$\log K^\circ_1$	n_1	$\log K^\circ_2$
MHist	6.878 (2)		2.772 (6)
Hist[a]	6.48		–
PolyMHist	7.53 (7)	1.49 (5)	2.0
MH2	7.66 (18)	1.29 (9)	2.5
PolyHist[a]	7.64	2.22	2.3
co-3	7.06 (6)	1.41 (6)	2.5
co-2	6.84 (6)	1.23 (7)	2.8
co-1	6.70 (12)	1.15 (12)	2.8
Poly(Hist-*co*-NIPAAm)[a]	7.11	1.76	2.9
	$\log K_1 = \log K^\circ_1 + (n_1 - 1)\log[(1 - \alpha)/\alpha]$		

[a]Values in parentheses are standard deviations. Ref. 6.

thermore, as the protonation of the imidazole nitrogen is concerned, the linear decreasing pattern of the logK_1, and also of the n_1, in relation to the MHist content in copolymers with NIPAAm, is a result of the increased distance between the charges along the chain. This reduces the electrostatic contribution of the charges and shows as the monomers are randomly distributed with a predominance of block-like NIPAAm units. Similar results were previously reported for vinyl related copolymers containing L-valine residues [30, 31]. In the latter case, the decreasing trend of the log$K$ for the acrylates was ascribed to the increased distance between the charges, while methacrylate compounds showed a closer homopolymer polyelectrolyte behaviour. A block-like distribution of the charged methacrylic units was hypothesized in view of their different monomeric structures. In the case of the poly (ampholyte)s, any increase of the uncharged NIPAAm units, leads to a decrease of the proton up-take by the basic imidazole nitrogen. The logK_1 decrease is always due to the lower decreased electrostaticity exerted by the charged carboxylate anions. When the MHist content is very low, the logK_1 value approaches that of the corresponding monomer. On the other hand, the protonation of the carboxylate group in the copolymers cannot be well depicted because of the low basicity constants. These values account only for a limited degree of protonation in the experimental condition of this study.

The viscometric data well support the protonation-like mechanism of the polymers containing MHist. Figure 7 shows the reduced viscosity pattern at different pHs of the homopolymer polyMHist, while Figure 8 shows the conformational behaviour of the corresponding three copolymers.

In all cases, the fully ionized macromolecule (L^-) is in the extended chain conformation. As the protonation of the basic imidazole nitrogen occurs, the coiling is sharp at pH close to the logK_1 and becomes the lowest at the maximum formation of the zwitterionic $L^{\pm}$ species. In the polyMHist, as the protonation proceeds, with the neutralization of the carboxylate anion, the coil dimension increases again for the presence of a net positive charge on the macromolecule (L^+). This trend, even if present in the copolymers co-3 and co-2, having relatively a greater amount of MHist content, was not shown in the copolymer co-1. Moreover, as the MHist

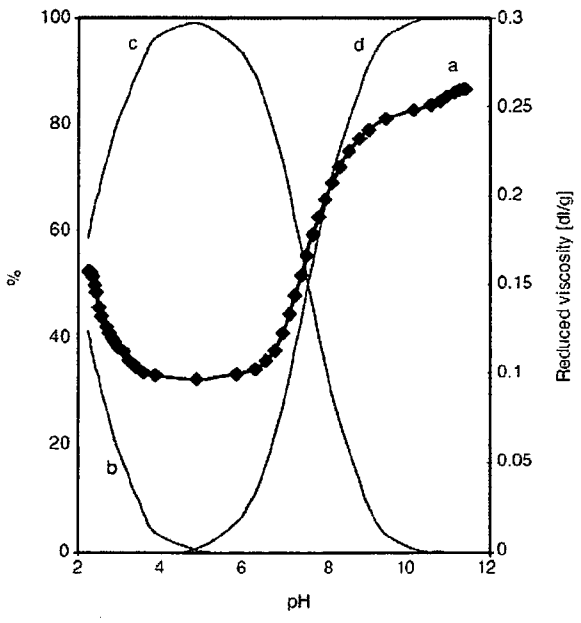

Figure 7. Reduced viscosity (η/C [dl/g]) of the polyMHist in relation to the pH (a) with the superimposed species distribution curves [%] obtained by the log$K$s evaluated at 25°C in 0.15M NaCl (b – di-protonated L^+; c – mono-protonated, zwitterionic $L^{\pm}$; d – un-protonated L^-, where L is the monomer unit of the polymer)

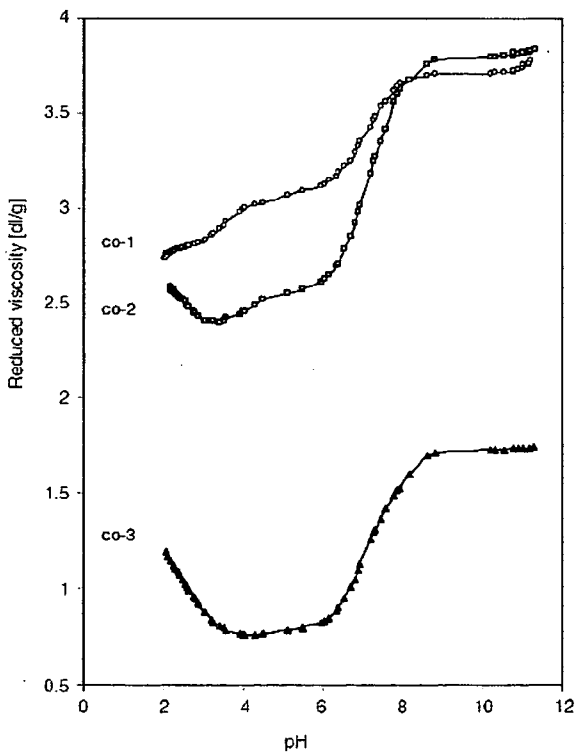

Figure 8. Reduced viscosity in relation to the pH for the poly(MHist-*co*-NIPAAm) copolymers at 25°C in 0.15M NaCl

content in the copolymers decreased, the lowest minimum of the reduced viscosity was shifted at lower pHs, with the disappearance in the *co*-1. Even if this behaviour seems to be quite interesting, the further collapse of the macromolecular coil at lower pH may be due to more competitive electrostatic-hydrophobic forces. During the protonation process, the polymer gradually uncoils, due to the increased electrostaticity of the protonated imidazole nitrogen. The hydrophobic forces between the isopropyl groups in NIPAAm are able to outweigh the repulsive electrostatic interactions when they are present at a critical concentration. A similar behaviour was already observed for vinyl poly (acid)s containing α-aminoacids with lateral isopropyl groups [30].

Enthalpy and entropy changes

The results of the calorimetric titrations revealed, for all the compounds considered, similar enthalpograms during the protonation of the basic groups present in the MHist moiety. The exothermic protonation reaction of the imidazole nitrogen revealed a well defined break-point corresponding to the amount of MHist close to that found by the potentiometry. The further protonation of the carboxylate anion showed a rather negligible endothermicity. Thus, we evaluated the enthalpy ($-\Delta H°$) and the entropy ($\Delta S°$) change values only for the imidazole nitrogen protonation (Table 6). The results of the methacrylate compounds (MHist and polymers containing MHist) showed rather similar protonation behaviour also when compared to the previously reported acrylate analogues [6].

Unlike the reported study on poly(Hist) [6], that showed a peculiar $-\Delta H°/\alpha$ plot and the protonation process of which was likely attributed to the formation of hydrogen bonds between adjacent monomer units, the poly(MHist) revealed a 'real' $-\Delta H°$ that was independent on the degree of protonation α. The different behaviour may be ascribed only to the presence of the further methyl group in the backbone macromolecular chain. Its hydrophobic character was evident in the greater $\Delta S°$ value of the MHist and the polyMHist when compared to the corresponding acrylate analogues [6]. However, the lower polyelectrolyte effect reported for the polyMHist during the protonation of the basic imidazole nitrogen is reflected in a lower $\Delta S°$ decrease on α, involving thus the release of further water molecules surrounding closer monomer units. In Figure 9 is reported the decreasing trend of $\Delta S°$ in relation to α for the protonation of the imidazole nitrogen in polyMHist and its copolymers with NIPAAm.

The trend is similar to that shown by the corresponding log*K*s, and, being the $-\Delta H°$ 'real' (i.e. independent on α), the polyelectrolyte effect is only attributed to entropy contributions. In fact, the protonation of the imidazole nitrogen led to a sharp decrease of the macromolecular coil with the for-

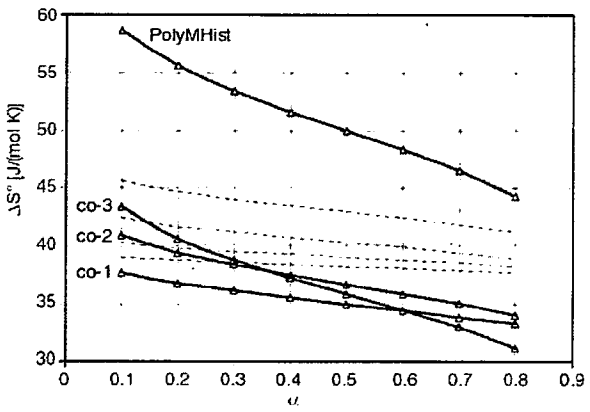

Figure 9. Entropy change ($\Delta S°$ [J/(mol·K)]) values in relation to α for the protonation of the imidazole nitrogen in polyMHist and related copolymers in 0.15M NaCl and 25°C. (Dotted lines refers to $-\Delta G°$ of the same compounds)

Table 6. Thermodynamic functions of the imidazole nitrogen protonation in vinyl compounds containing L-histidine residues (25°C in 0.15M NaCl)

Compd	$-\Delta G°$, [kJ/mol]	$-\Delta H°$, [kJ/mol]	$\Delta S°$, [J/(mol·K)]	Ref.
MHist	39.26 (1)	29.3 (2)	33.4 (7)	This work
Hist	37.0	30.5	21.8	[6]
PolyMHist	43.0 (4)	28.1 (4)	50 (1)	This work
PolyHist	43.6	30.6	44	[6]
co-3	40.3 (3)	29.6 (6)	36 (2)	This work
co-2	39.0 (3)	28.1 (6)	37 (2)	This work
co-1	38.2 (7)	28.7 (7)	35 (2)	This work
Poly(Hist-*co*-NIPAAm)	40.6	29.5	37	[6]

mation of zwitterionic species. Besides the likely ordering to some extend of the zwitterions, the process led to a release of water molecules because the macromolecule becomes tightly coiled. This was seen in some cases because phase separation occurred at the isoelectric point. As a matter of fact, the corresponding hydrogels decreased their degree of swelling for the loss of water molecules.

3.3. Swelling behaviour of hydrogels

The swelling behaviour of the hydrogels was studied in relation to the pH, the temperature, the electric current, and the concentration of the simple NaCl salt at pH 9, i.e. in the completely ionized form of the MHist units. The sample slabs swelling kinetics for the two different cross-linked CMH2 and CMH10 hydrogels was recorded at constant ionic strength (0.15M NaCl) and at two different pHs (1.9 and 8.8). The results, reported in Figure 10, show the different hydration ability in the different pH conditions. It is evident that the degree of swelling (DS) is greater for the less cross-linked CMH2 gel and at higher pHs. In both cases, the equilibrium DS was reached within few hours. Both the gels are friable in the dry state and become transparent as the water content increases.

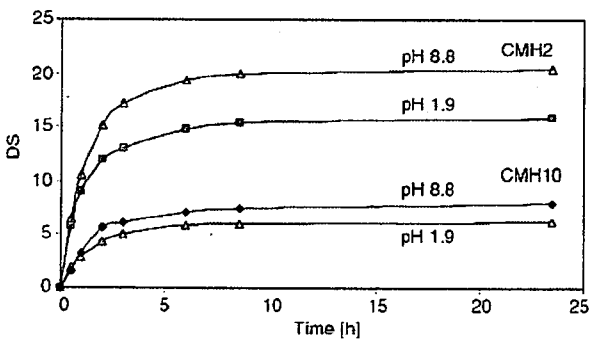

Figure 10. Swelling kinetics of the hydrogels CMH2 (slabs of 50 mg) and CMH10 (slabs of 55 mg) at two different pHs in 0.15M NaCl and 24°C

Effect of pH, temperature, ionic strength, and electric current

The swelling behaviour of the hydrogel MH2 in relation to pH, at 25°C in 0.15M NaCl, is reported in Figure 11. The EDS/pH plot, being similar to that reported for the viscometric data of polyMHist in Figure 7, sensitively reveals a decreasing pattern by increasing the pH in the narrow range 4 to 6. In

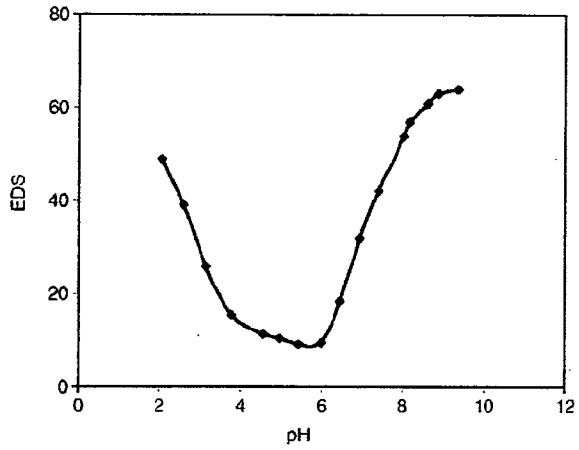

Figure 11. Equilibrium degree of swelling (EDS) in relation to the pH of the gel MH2 in 0.15M NaCl at 25°C

this pH-range the zwitterionic form predominates with its maximum at the isoelectric point (i.p., pH 5). It is likely that the greater log$K$ values of the hydrogel, with its lower polyelectrolyte behaviour, may lead to more stable ionized species of greater hydrophilic quality. As the pH shifts-out from this range, the gel MH2 swells as a consequence of its water content increase, due to the predominance of net positive or negative charges.

On the other hand, the hydrogel CMH2 behaves likewise the copolymer co-2, having the latter a similar comonomer composition. In Figure 12 the EDS/pH profile of the hydrogel CMH2 at 25°C in 0.15M NaCl is reported. Compared to the previously reported acrylate CH1 hydrogel containing Hist [19], the lower EDS value is due to the greater cross-link density in CMH2. The striking similarity of the swelling behaviour with the reduced viscos-

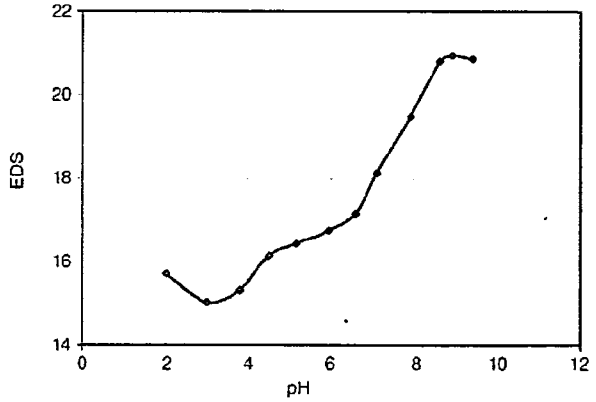

Figure 12. Equilibrium degree of swelling (EDS) in relation to the pH of the gel CMH2 in 0.15M NaCl at 25°C

ity (Figure 8) suggests a similar polyelectrolyte behaviour of the two polymers, even in the different free and cross-linked forms. On the basis of these results it is likely to hypothesize any tailoring hydrogel system to collapse at desired pHs, by introducing the right amount of the two co-monomers. Of course, if in these copolymers the MHist content becomes less than a critical value (about 5 mol%), the polyampholyte quality vanishes because of the superimposing effect of the hydrophobic interactions exerted by the isopropyl groups of the NIPAAm moieties.

As regards the effect of the temperature, Figure 13 shows the swelling behaviour of the CMH2 hydrogel in a wide range of temperatures. The hydrogel swelling was studied in 0.15M NaCl and in three different buffered solutions of significant pHs.

Any increase of the temperature resulted in a deswelling ability of the hydrogel. It retained its hydration state at high as well as at low pHs. Contrary to the previously reported acrylate hydrogel CH1 [19], the CMH2 hydrogel showed a phase separation at higher temperatures and at lower pHs. The presence of the hydrophobic MHist unit, instead of decreasing the LCST (Lower Critical Solution Temperature) [40] of the NIPAAm based hydrogels (32°C), revealed a greater temperature increase. This point will be better investigated even though the behaviour may be further on ascribed to the peculiar protonation mechanism of the MHist based hydrogels. A similar greater increase of the phase separation temperature was observed for the soluble copolymers. In Figure 14 is reported the relationship between the viscometric data and the temperature (in the range 25–46°C) of the three copolymers (co-1, co-2, and co-3) at the three significant pHs (9, most negatively ionized; 5, zwitterionic; 2, most positively ionized).

Unlike the straight line observed in all cases by co-3, the copolymer co-2 showed an increased negative line slope at pH 5, close to 38°C; on the other hand, the co-1 showed more negative line slopes at different temperatures, depending on the pH. Table 7 summarizes the obtained results. The observed differences are due to the different content of the MHist units in the copolymers; lower MHist content displayed greater responsiveness to pH and temperature. It is worthwhile noting the

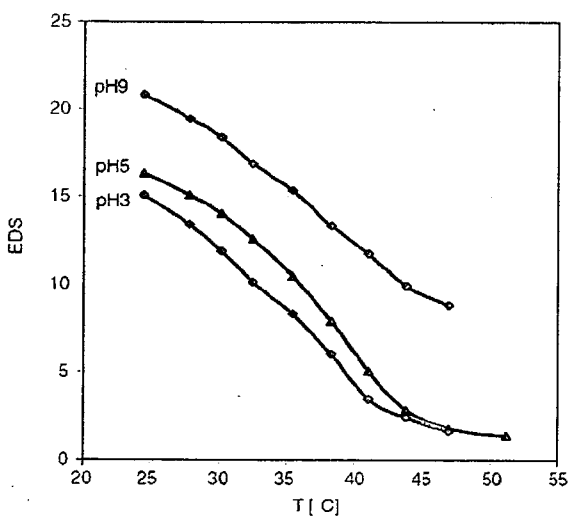

Figure 13. EDS of the gel CMH2 in relation to the temperature [°C] at three different pHs in 0.15M NaCl

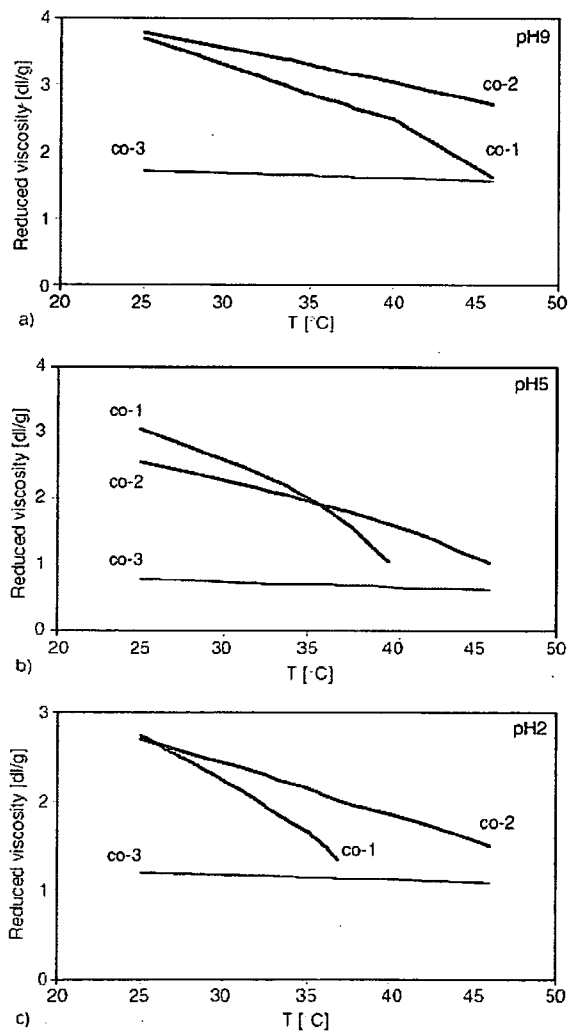

Figure 14. Reduced viscosity (η/C [dl/g]) of the three copolymers (co-1, red curves; co-2, green curves; co-3, blue curves) in relation to the temperature at three different pHs (9, 5 and 2) in 0.15M NaCl

Table 7. Straight line parameters from the reduced viscosity values of the three copolymers co-1, co-2, and co-3

Copolymer	pH	Line slope	R^2	Range of temperatures [°C]
co-3	2	–0.0054	0.990	25–46
	5	–0.0074	0.989	25–46
	9	–0.0079	0.995	25–46
co-2	2	–0.057	0.999	25–46
	5	–0.072	0.982	25–46
	5	–0.061	0.998	25–38
	5	–0.094	0.995	38–46
	9	–0.052	0.999	25–46
co-1	2	–0.115	0.994	25–46
	2	–0.109	0.998	25–35
	2	–0.166	0.993	35–37
	5	–0.126	0.964	25–46
	5	–0.105	0.996	25–35.5
	5	–0.205	0.997	35.5–46
	9	–0.096	0.981	25–46
	9	–0.083	0.999	25–40
	9	–0.146	0.999	40–46

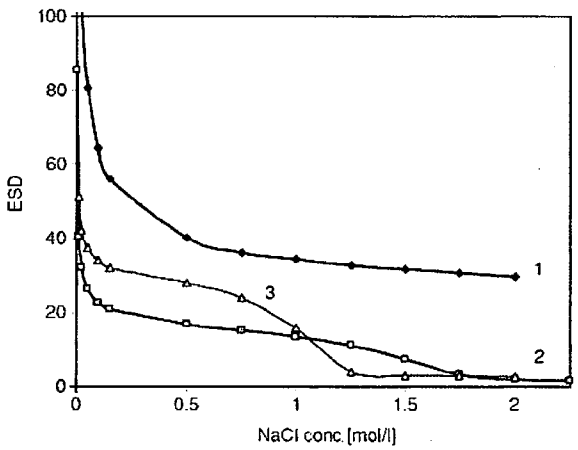

Figure 15. EDS of gels MH2 (1), CMH2 (2), and CH1 (3) [19] in relation to the concentration of NaCl (pH 9 and 25°C)

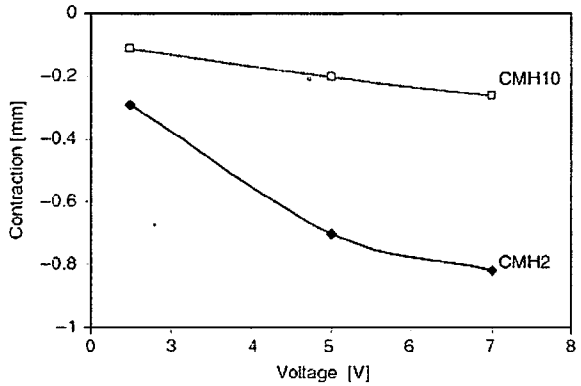

Figure 16. Hydrogel contraction [mm] in relation to the electric stimulation (2.5, 5.0, and 7.0 V) at 10 minutes elapsed time and pH 9

similar behaviour between the viscosity of the soluble co-1 and the EDS of the cross-linked gel CMH2 (Figure 13), having both the compounds similar MHist content. At the three different pHs, either the reduced viscosity and the EDS values follow the same trend and collapse almost at the same temperatures.

Moreover, the effect of the ionic strength, i.e. the concentration of sodium chloride, on the swelling properties of the MH2 and CMH2 hydrogels at pH 9, is reported in Figure 15 along with the results previously obtained with the gel CH1 [19], for comparison.

Unlike the hydrogel MH2, which shows only polyelectrolyte behaviour for the shielding effect of the carboxylate groups negative charges, the CMH2 showed a volume phase transition phenomenon at a NaCl concentration of 1.75 mol/l. This concentration resulted greater than that shown by the Hist-based CH1 hydrogel [19].

The electric current effect on the two hydrogels is reported in Figure 16. Any increase of the applied potential linearly increased the gel contraction. Moreover, the contraction of the gel CMH2 was higher than that of CMH10, because of the lower cross-links amount. These results, although more effective, are in agreement with the previously reported ones on the gels containing the acrylate Hist analogues.

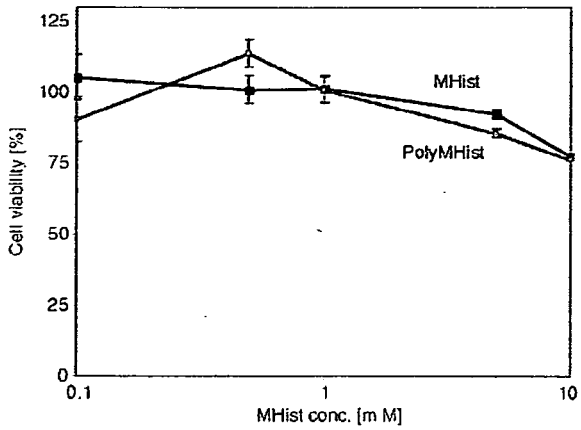

Figure 17. Cytotoxicity of the MHist and poly(MHist) against MC3T3-E1 (mouse osteoblast) cells

3.4. In vitro cytotoxicity

The cytotoxic effect of the poly(MHist) was evaluated by the cell culture of osteoblasts from mouse (MC3T3-E1). Figure 17 shows the cell proliferation in the presence of the polymer and its low-molecular weight precursor.

It is noticeable that no significant cytotoxicity was observed for two days at concentration up to 5 mM. Thus, these zwitterionic compounds in the cross-linked hydrogel form may show potential applications in bone resorption when implanted in specific tissues, for the releasing of loaded amino-bisphosphonate drugs [17].

4. Conclusions

This paper, concerning with our research interest on poly(ampholyte)s [6, 19, 41], developed a thermodynamic study for the protonation of basic groups in the free and cross-linked methacrylate polymers carrying the L-histidine residues. As a rule, methacrylate polyelectrolytes, particularly poly(carboxyl acid)s, show more complex thermodynamic data than the corresponding acrylates [42]. In the case of poly(ampholyte)s, the more hydrophobic character of the main polymer chain was evident in both the free and the cross-linked hydrogels. Unlike the corresponding acrylate, these new ligands show a lower polyelectrolyte behaviour. The 'real' enthalpy changes and the lower n values of the modified Henderson-Hasselbalch equation are the two main thermodynamic data showing the difference. Moreover, the volume phase transition behaviour of the hydrogels, based on the pH-responsive poly(ampholyte)s and on the temperature-responsive *N*-isopropylacrylamide, revealed that the thermodynamic data are close to the soluble analogues ones. The LCST of the polyNIPAAm, that is close to the body temperature, may be tuned by the pH and the proper amount of the purposely synthesized ampholyte monomer. Thermodynamic and biological characterization, along with the salt-induced phase transition and the dc electroshrinking phenomenon shown by the methacrylate hydrogels, are indicative of a suitability of these materials for tissue engineering applications [15]. The increasing hydrophobic character makes some poly(ampholyte)s suitable for the preparation of nonbiofouling surfaces against proteins and cells [22].

Acknowledgements

The research work was supported by a grant of the Italian MIUR, as a project within PRIN 2004, and by a grant of the PAR 2005 (Siena University). Thanks are due to Miss Ilaria Casolaro for having carefully read the manuscript.

References

[1] Casolaro M.: Stimuli-responsive polymers (thermodynamics in drug delivery technology). in 'Polymeric Materials Encyclopedia' (Ed.: Salamone J. C.), CRC Press, Boca Raton, vol. **10**, 7979–7992 (1996).

[2] Casolaro M., Paccagnini E., Mendichi R., Ito Y.: Stimuli-responsive polymers based on L-phenylalanine residues: the protonation thermodynamics of free polymers and cross-linked hydrogels. Macromolecules, **38**, 2460–2468 (2005).

[3] Barbucci R., Casolaro M., Magnani A.: Ionic and ionizable synthetic polymers: interactions in aqueous solution. Coordination Chemistry Reviews, **120**, 29–50 (1992).

[4] Casolaro M.: Thermodynamics of multiple-responsive polyelectrolytes with complexing ability towards the copper(II) ion. Reactive Polymers, **23**, 71–83 (1994).

[5] Bignotti F., Penco M., Sartore L., Peroni I., Mendichi R., Casolaro M., D'Amore A.: Synthesis, characterization and solution behaviour of intelligent polymers bearing L-leucine residues in the side chains. Polymer, **41**, 8247–8256 (2000).

[6] Casolaro M., Bottari S., Cappelli A., Mendichi R., Ito Y.: Vinyl polymers based on L-histidine residues. Part 1.: The thermodynamics of poly(ampholyte)s in the free and in the cross-linked gel form. Biomacromolecules, **5**, 1325–1332 (2004).

[7] Cho I., Shin J-S.: Hydrophobic and ionic interactions in the ester hydrolysis by imidazole-containing polymers. Bulletin of Korean Chemical Society, **3**, 34–36 (1982).

[8] Bertini I., Scozzafava A.: Copper(II) as probe in substituted metalloproteins. in 'Metal ions in biological systems' (Ed.: Sigel H.) Marcel Dekker, New York, **12**, 31–74 (1981).

[9] Kowalik-Jankowska T., Ruta-Dolejsz M., Wisniewska K., Lankiewicz L., Kozlowski H.: Copper(II) complexation by human and mouse fragments (11–16) of β-amiloid peptide. Journal of the Chemical Society, Dalton Transactions, 4511–4519 (2000).

[10] Aronoff-Spencer E., Burns C. S., Avdievich N. I., Gerfen G. J., Peisach J., Antholine W. E., Ball H. L., Cohen F. E., Prusiner S., Millhauser G. L.: Identification of the Cu^{2+} binding sites in the N-terminal domain of the prion protein by EPR and CD spectroscopy. Biochemistry, **39**, 13760–13771 (2000).

[11] Kumar A., Kamihira M., Galaev I. Y., Iijima S., Mattiasson B.: Binding of Cu(II)-poly(*N*-isopropylacrylamide)/vinylimidazole copolymer to histidine-tagged protein: a surface plasmon resonance study. Langmuir, **16**, 865–871 (2003).

[12] Kumar A., Wahlund P-O., Kepka C., Galaev I. Y., Mattiasson B.: Purification of histidine-tagged single-chain Fv-antibody fragments by metal chelate affinity precipitation using thermoresponsive copolymers. Biotechnology and Bioengineering, **84**, 494–503 (2003).

[13] Carter S., Rimmer S., Sturdy A., Webb M.: Highly branched stimuli responsive poly[(*N*-isopropylacrylamide)-co-(1,2-propandiol-3-methacrylate)]s with protein binding functionality. Macromolecular Bioscience, **5**, 373–378 (2005).

[14] Carter S., Rimmer S., Rutkaite R., Swanson L., Fairclough J. P. A., Sturdy A., Webb M.: Highly branched poly(*N*-isopropylacrylamide) for use in protein purification. Biomacromolecules, **7**, 1124–1130 (2006).

[15] Stile R. A., Burghardt W. R., Healy K. E.: Synthesis and characterization of injectable poly(*N*-isopropylacrylamide)-based hydrogels that support tissue formation in vitro. Macromolecules, **32**, 7370–7379 (1999).

[16] Cini R., Defazio S., Tamasi G., Casolaro M., Messori L., Casini A., Morpurgo M., Hursthouse M.: *fac*-$(Ru(CO)_3)^{2+}$-core complexes and design of metal-based drugs. Synthesis, structure, and reactivity of Ru-thiazole derivative with serum proteins and absorption-release studies with acryloyl and silica hydrogels as carriers in physiological media. Inorganic Chemistry, **46**, 79–92 (2007).

[17] Casolaro M., Casolaro I., Spreafico A., Capperucci C., Frediani B., Marcolongo R., Margiotta N., Ostuni R., Mendichi R., Samperi F., Ishii T., Ito Y.: Novel therapeutic agents for bone resorption. Part 1. Synthesis and protonation thermodynamics of poly(amidoamine)s containing bis-phosphonate residues. Biomacromolecules, **7**, 3417–3427 (2006).

[18] Lin J. H.: Bisphosphonates: A review of their pharmacokinetic properties. Bone, **18**, 75–85 (1996).

[19] Casolaro M., Bottari S., Ito Y.: Vinyl polymers based on L-histidine residues. Part 2. The swelling and electric behaviour of smart poly(ampholyte) hydrogels for biomedical applications. Biomacromolecules, **7**, 1439–1448 (2006).

[20] Nitschke M., Götze T., Gramm S., Werner C.: Detachment of human endothelial cell sheets from thermoresponsive poly(NiPAAm-co-DEGMA) carriers. Express Polymer Letters, **1**, 660–666 (2007).

[21] Morcellet-Sauvage J., Morcellet M., Loucheux C.: Polymethacrylic acid derivatives. 1. Preparation, characterization, and potentiometric study of poly(*N*-metacryloyl-L-alanine-co-N-phenylmethacrylamide). Die Makromolekulare Chemie, **182**, 949–963 (1981).

[22] Ishii T., Wada A., Tsuzuki S., Casolaro M., Ito Y.: Copolymers including L-histidine and hydrophobic moiety for preparation of nonbiofouling surface. Biomacromolecules, **8**, 3340–3344 (2007).

[23] Okamoto Y.: Hydrolyses of α-amino acid p-nitrophenyl esters by poly(*N*-methacryloyl-L-histidine) (in Japanese). Journal of The Chemical Society of Japan, **6**, 870–873 (1978).

[24] Iwakura Y., Toda F., Suzuki H.: Synthesis of *N*-[1-(1-substituted 2-oxopropyl)]acrylamides and -methylacrylamides. Isolation and some reactions of intermediates of the Daikin-West reaction. Journal of Organic Chemistry, **32**, 440–443 (1967).

[25] Rempp P., Merrill E. W.: Polymer synthesis. Huthig and Wepf, Basel (1991).

[26] Penco M., Bignotti F., Sartore L., Peroni I., Casolaro M., D'Amore A.: Stimuli-responsive polymers based on *N*-isopropylacrylamide and *N*-methacryloyl-L-leucine. Macromolecular Chemistry and Physics, **202**, 1150–1155 (2001).

[27] Barbucci R., Casolaro M., Danzo N., Barone V., Ferruti P., Angeloni A.: Effect of different shielding groups on polyelectrolyte behaviour of polyamines. Macromolecules, **16**, 456–462 (1983).

[28] Gans P., Sabatini A., Vacca A.: Superquad: an improved general program for computation of formation constants from potentiometric data. Journal of the Chemical Society, Dalton Transactions, 1195–1200 (1985).

[29] Ishiyama M., Tominaga H., Shiga M., Sasamoto K., Ohkura Y., Ueno K.: A combined assay of cell viability and in vitro cytotoxicity with a highly water-soluble tetrazolium salt, neutral red and crystal violet. Biological and Pharmaceutical Bulletin, **19**, 1518–1520 (1996).

[30] Casolaro M.: Vinyl polymers containing L-valine and L-leucine residues: thermodynamic behaviour of homopolymers and copolymers with *N*-isopropylacrylamide. Macromolecules, **28**, 2351–2358 (1995).

[31] Casolaro M., Barbucci R.: Thermodynamic behaviour of polyelectrolytes with the lower critical solution temperature (LCST) phenomena. Polymers for Advanced Technologies, **7**, 831–838 (1996).

[32] Casolaro M.: Intelligent polymer systems for molecular separation and controlled delivery of drugs. In 'Frontiers in biomedical polymer applications' (Ed.: Ottenbrite R. M.) Technomic Publishing Co. Inc., Lancaster, Vol. 1, 109–122 (1998).

[33] Montaudo G., Montaudo M. S.: Polymer characterization methods. in 'Mass Spectrometry of Polymers' (Eds.: Montaudo G., Lattimer R. P.) CRC Press, Boca Raton, 41–111 (2002).

[34] Montaudo G., Montaudo M. S., Samperi F.: Matrix-assisted laser desorption ionization/mass spectrometry of polymers (MALDI-MS). in 'Mass Spectrometry of Polymers' (Eds.: Montaudo G., Lattimer R. P.) CRC Press, Boca Raton, 419–521 (2002).

[35] Montaudo G., Samperi F., Montaudo M. S.: Characterization of synthetic polymers by MALDI-MS. Progress in Polymer Science, **31**, 277–357 (2006).

[36] Morawetz H.: Macromolecules in Solution, Wiley-Interscience, New York (1980).

[37] Katchalsky A., Spitnik P.: Potentiometric titrations of polymethacrylic acid. Journal of Polymer Science, **2**, 432–446 (1947).

[38] Murai N., Sugai S.: Side-chain effect on conformation of ionizable polypeptides in aqueous solution. Biopolymers, **13**, 1161–1171 (1974).

[39] Barbucci R., Casolaro M., Magnani A., Roncolini C.: Different protonation behaviour of two poly (methacrylic acid) derivatives containing *N*-acyl-glycine and *N*-acyl-β-alanine residues: Thermodynamic and FT-IR studies. Macromolecules, **24**, 1249–1257 (1991).

[40] Schild H. G., Tirrel D. A.: Microcalorimetric detection of lower critical solution temperatures in aqueous polymer solutions. The Journal of Physical Chemistry, **94**, 4352–4356 (1990).

[41] Kudaibergenov S. E.: Polyampholytes: synthesis, characterization and application. Kluwer Academic, New York (2002).

[42] Bekturov E. A., Bakauova Z. Kh.: Synthetic water-soluble polymers in solution. Huethig and Wepf Verlag, Basel (1986).

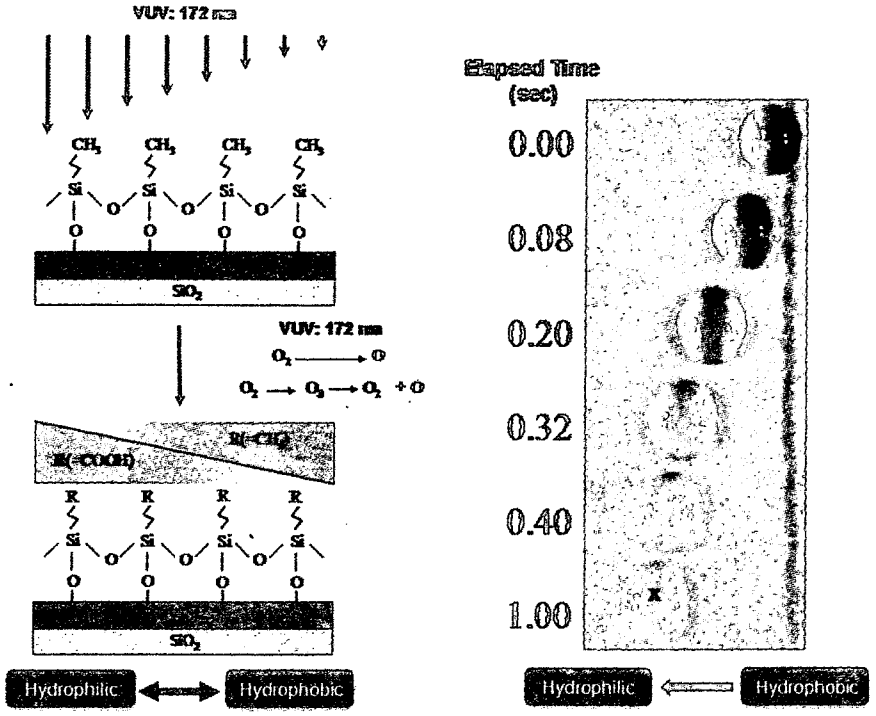

Control of Water Droplet Movement

Yoshihiro ITO
y-ito@riken.jp
Nano Med. Eng. Lab., RIKEN

A hydrophobic to hydrophilic gradient surface was prepared using the tuned photodegradation of an alkylsilane self-assembled monolayer (SAM) using irradiation of vacuum ultraviolet light (wavelength＝172 nm). The water contact angle on the photo-degraded SAM surface was adjusted using the intensity and time photo-irradiation parameters. The water drop moved from the hydrophobic to hydrophilic surface with a velocity that depended on the gradient. The higher the gradient, the faster the water moved. For the first time, we have prepared a gradient surface using photodegradation where the movement of a water drop was regulated by the degree of gradation.

Polymer Preprints, Japan **2007**, *56*, 1532.

総説（Review Article）：膜（MEMBRANE），32（5），276-280（2007）

●特集｜人工膜関連シンポジウム「膜を用いた新しい細胞培養操作」

再生医療のための幹細胞増幅基材

伊藤嘉浩

理化学研究所　伊藤ナノ医工学研究室　〒351-0198 埼玉県和光市広沢2-1

Biomaterials to *Ex Vivo* Expand Stem Cells for Regenerative Medicine

Yoshihiro Ito

Nano Medical Engineering Laboratory, RIKEN, 2-1 Hirosawa, Wako-shi, Saitama 351-0198, Japan

For achievement of regenerative medicine, *ex vivo* expansion of stem cells which can be differentiated to various cells is very important. However, it is very difficult to efficiently and safely culture some stem cells such as hematopoietic stem cells in cord blood or human embryonic stem cells. Therefore, the culture systems are investigated by many researchers. Here the state-of-arts of culture of stem cells and in particle development of biomaterials for expansion of stem cells is discussed.

Key words : cell culture／stem cell／biomaterial／immobilization／growth factor／nurse cell

1. はじめに

これまで半世紀にわたり，人類は病気で機能障害や機能不全に陥った生体組織・臓器の治療のために近代的な人工臓器や臓器移植を発展させてきた（Fig. 1）．しかし，人工臓器はまだまだ不備が多く，臓器移植ではドナーの不足が深刻である．そこで最近「再生医療」という細胞を積極的に利用して，生体機能の再生をはかる医療が考えられるようになった．再生医療は，1997年のクローン羊の出現や1998年のヒト胚性幹（ES）細胞の樹立から注目を集めるようになった．再生医療では，ES細胞ばかりでなく，成人の体のなかにも体性幹細胞が存在することがわかり，一部はすでに医療に用いられ，今後その治療用途はますます拡大してゆくと考えられている（Fig. 2）．このような医療の実現のための一つの大きな課題は，非常に僅かしかない幹細胞を未分化状態のまま効率よく増やすことである[1~9]．

我々は，これまで成長因子やサイトカイン固定化材料が細胞培養に応用できることを示してきた[10~14]．もしこのような基材を用いて，再生医療で重要となるヒト幹細胞を，安全かつ迅速に供給できるようにするバイオリアクターが開発できればと考えた．これまで，生体外での細胞培養は長い歴史をもち，この技術により生命科学は飛躍的な進歩を遂げてきた．今や実験手段として細胞培養は日常的で不可欠な技術になっているが，通常は，動物から採取した血清を用い，場合によっては異種動物由来の細胞を培養液に共存させて行われている．しかし，ヒト幹細胞を培養し，医療に用いるためには，安全な培養が最も重要である．異種動物由来の血清や細胞の使用は，これまでしばしば指摘され問題になってきたようにウイルスやプリオン感染，さらに未知の病原体による感染を招く恐れがある．そこで，これら異種動物由来の生体成分を混在させない完全な人工幹細胞培養系を確立することが必須となる．

2. 化学固定化保育細胞による培養システムの開発

白血病治療は，骨髄移植，末梢血幹細胞移植から，

Tel : 048-467-5809　Fax : 048-467-9300
E-mail : y-ito@riken.jp

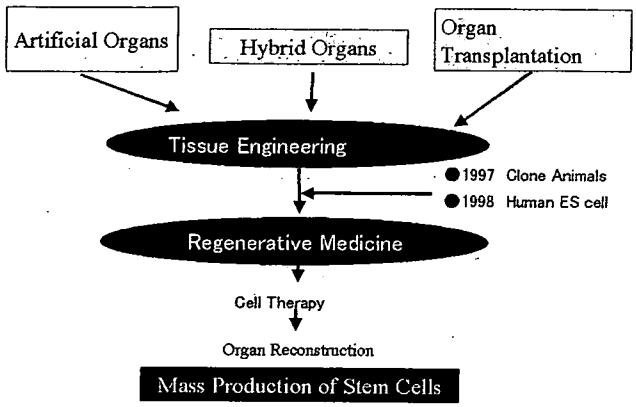

Fig. 1 History to regenerative medicine.

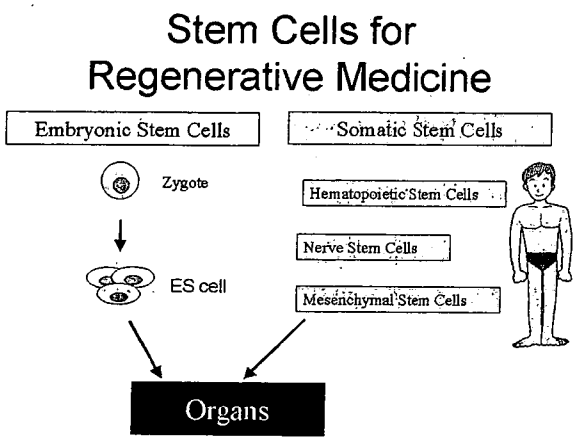

Fig. 2 Stem cells for regenerative medicine.

臍帯血移植へと展開されてきた．臍帯血は，これまで廃棄されていたものを使用できる上に，組織適合性が寛容で冷凍保存も可能で今後の発展が期待されている．しかし一般に採取可能な臍帯血からは充分量の造血幹細胞が得られず，成人の治療には困難が伴っている．また，ヒトES細胞培養で動物由来血清や保育細胞を使用している場合，ヒト型でない化学修飾が起きるという報告が近年明らかにされた．そのため，これら幹細胞を異種動物由来成分を含まずに培養することが，望まれる．

我々は，まず国立がんセンターとの共同研究で，ヒト骨髄間葉系幹細胞（hMSC）の不死化をヒトテロメラーゼ逆転写酵素（hTERT）遺伝子導入により行い，これを保育細胞として用いた（Fig. 3）．不死化により株化細胞のようにhMSCが扱いやすくなった．さらに，不死化hMSCをアルデヒド基をもつ化合物で架橋固定化してもヒト臍帯血造血幹細胞の増幅支持能があることがわかった．特にグルタルアルデヒドで固定化した保育細胞は高い活性があり，長期的に冷蔵保存可能であることがわかった．さらには凍

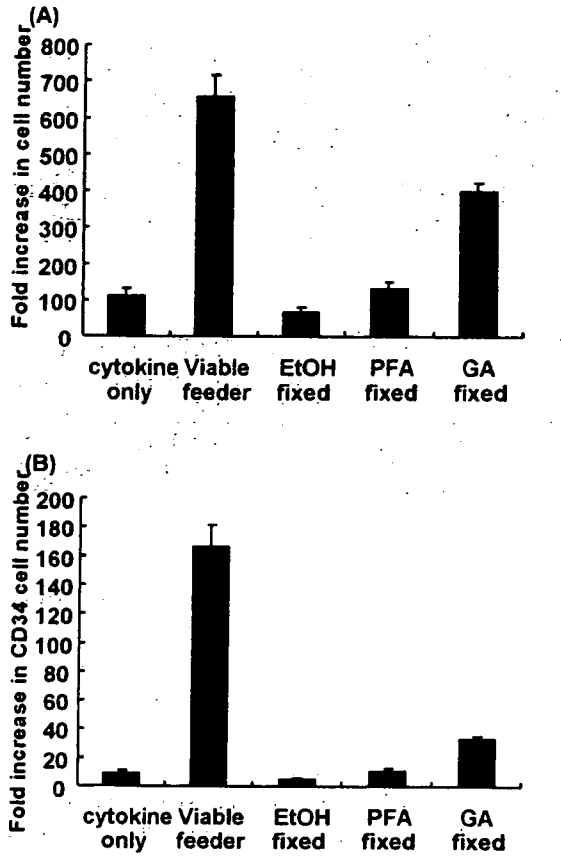

Fig. 3 *Ex vivo* expansion of (A) total cells and (B) $CD34^+$ (hematopoietic stem) cells in human cord blood. EtOH, PFA, and GA mean ethanol, paraformaldehyde, and glutaraldehyde, respectively. Viable feeder means non-fixed nurse cell.

結乾燥して保存しても，未分化状態の造血幹細胞の体外増幅支持に活性があることもわかった．凍結乾燥しても活性を保持できることから，保存性の高い利用しやすい基材とすることができた[15]．

一方，霊長類ES細胞培養のためには，医療廃棄物として捨てられる胎盤からヒト羊膜上皮細胞を採取し，保育細胞となることを見出した[16]．これについても国立がんセンターとの共同研究でhTERT導入により不死化し，その上で化学固定して培養用基材とする検討を行った．その結果，グルタルアルデヒドやホルムアルデヒドで固定化した不死化ヒト羊膜上皮細胞も，サルES細胞の未分化状態での増殖を支持することがわかった（Fig. 4）．さらに，化学固定化細胞はそのまま凍結乾燥保存できることや，一旦培養に用いた化学固定化細胞は，培養したES細胞をトリプシン処理して剥がしてから再度利用できることもわかった[17]．通常，保育細胞は，培養したい細胞の培養の時期にあわせて培養する必要があり，手間がかかったが，本研究のような化学固定化細胞を用

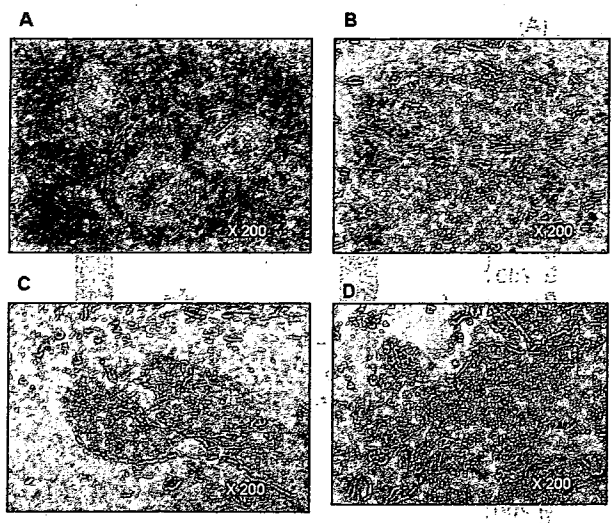

Fig. 4 Monkey embryonic stem (ES) cells on (A) primary mouse embryonic fibroblast treated with mitomycine-C, (B) human amniotic epithelial cells treated with 2.5% glutaraldehyde, (C) human amniotic epithelial cells treated with 2.5% formaline, and (D) coated gelatin were cultured, and they were stained with alkali phosphatase activity. On (A), (B), and (C) the monkey ES cells were stained but not on (D). This result indicated that ES cells grew with undifferentiated state on (A), (B), and (C).

いれば，そのような手間が省け，有用と考えられる．

3. 成長因子固定化材料の開発

再生医療では，幹細胞と，成長因子，そしてマトリックスが重要な因子となることが知られている．我々は，成長因子とマトリックスを組み合わせた新しい再生医療材料の開発を長年行ってきた．その主たる方法は，化学的手法によるもので，1990年代前半は，材料表面にカルボキシル基のような官能基を提示させ，そこに成長因子を固定化する手法を主に用いてきたが，1990年代後半からは，光リソグラフィ法による固定化を主に用いるようになった．これは特定の官能基を必要としないこと，マイクロパターン状固定化が簡単に行え，固定化成長因子の作用を顕微鏡下で視覚的に容易に観測できることから採用した．そして，インシュリン，上皮細胞成長因子（EGF），神経細胞成長因子（NGF），血管内皮細胞成長因子（VEGF）[18] などを固定化し，固定化領域で細胞成長や分化を制御できることを見出すとともに，固定化成長因子は細胞内に取り込まれずにダウン・レギュレーションを抑制し，刺激効果が高いことを明らかにしてきた（Fig. 5）．最近では，この他にも

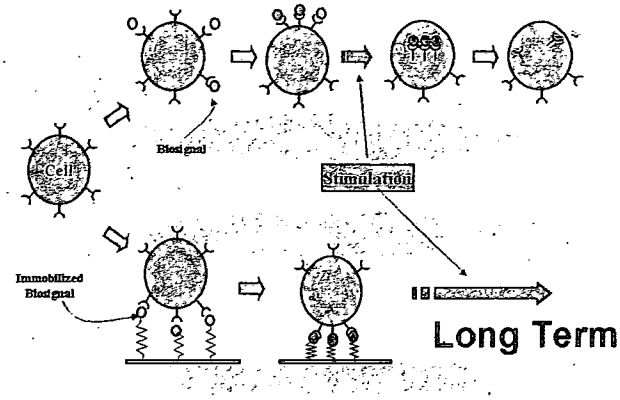

Fig. 5 Interactions of a soluble (above) and an immobilized (below) biosignal molecule. When a soluble biosignal molecule interacts with the cognate receptor, a complex is formed and the complexes are aggregated on the cell membrane. Subsequently the complexes are internalized and decomposed in the cell. The final process is called down-regulation and the mechanism contributes the reduction of overloading of stimulation by decreasing the number of receptors on the cell membrane. If the biosignal molecule is immobilized on materials, this down-regulation process is considered to be inhibited and stimulation will continue for a long time.

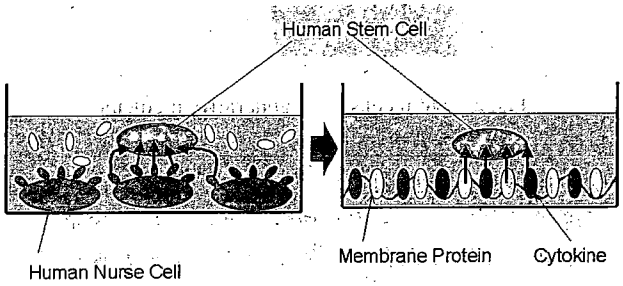

Fig. 6 Culture of human stem cells not in the presence of human nurse cells but on artificial protein layer composed of membrane proteins of nurse cells and cytokines in culture medium is desirable for future.

様々な成長因子が固定化され，その効果が実証されるようになってきている[14]．

上述の化学固定化保育細胞が幹細胞増幅活性をもつことから，Fig. 6に示すように保育細胞の膜タンパク質を固定化すれば同等の効果をもつ完全な人工膜を作出でき，より安全性が高く大量生産可能になると考えられる．そこで，いくつかのタンパク質固定化材料を新たに調製して造血幹細胞あるいはそのモデルとなる血球系細胞の培養を行い，その効果を検討した．その中で，エリスロポエチンをマイクロパターン状に固定化した材料を作成し，その上でUT7-

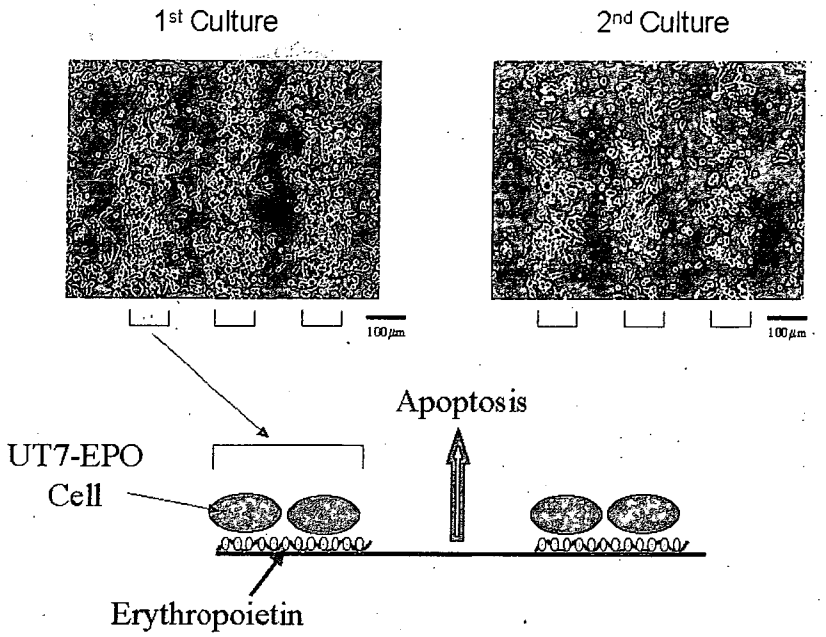

Fig. 7 Culture of erythropoietin-dependent UT7 (UT7-EPO) cells on erythropoietin-micropattern-immobilized surface. Although apoptosis was induced on the cells on non-immobilized surface, the cells on immobilized surface survived. In addition, the micropattern-immobilized surface can be used for second culture of cells.

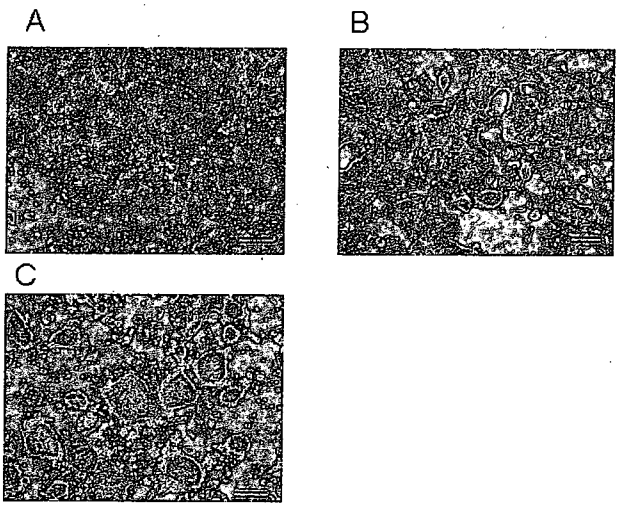

Fig. 8 Culture of mouse embryonic stem (ES) cells (A) in the absence of leukemia inhibitory factor (LIF), (B) in the presence of soluble LIF, and (C) in the presence of immobilized LIF and stained with alkali phosphatase activity. Although in (A) the cells were not so stained, in (B) and (C) the cells were stained. This result indicates that LIF was active for keeping undifferentiated growth of mouse ES cells in the soluble and immobilized states. Bars represent 200 μ m.

EPO細胞（エリスロポエチン依存性白血病細胞）を培養すると固定化領域でだけ細胞の増殖が観測され，非固定化領域ではアポトーシスが誘導される結果となり，固定化サイトカインの有効性を示すことができた（Fig. 7）[19]．また，造血幹細胞増幅と同様，ES細胞培養用にタンパク質の固定化による培養基材の開発を目指した研究も行った．マウスES細胞の培養のためには白血病抑制因子（LIF）と呼ばれるタンパク質を培養液に添加して未分化状態を保持することが行われるが，これを固定化しても活性を保持することを見出した（Fig. 8）[20]．

4. 課題及び今後の展望

保育細胞を化学固定化して基材として実際の幹細胞の増幅促進までは行うことができたが，タンパク質の固定化だけでは，実際の幹細胞の増殖促進までには至っていない．これは，幹細胞のニッチェ（周辺環境）に関する科学がまだ十分に理解されておらず，工学的にアプローチできる手段や分子情報が限られていることによる．そのため，幹細胞増幅活性をもつ保育細胞から膜タンパク質を探索することが必要である．再生医療の発展のために切実に望まれる技術であることから，今後も生命科学研究者との連携をさらに密にして展開することが重要である．

謝　辞

本研究は，財団法人神奈川科学技術アカデミーの

伊藤「再生医療バイオリアクター」プロジェクトの研究の一環として行われた．財団からの物心両面からの援助に感謝します．

文　献

1) 伊藤嘉浩：分子細胞療法, **2**, 52-55 (2003)
2) 伊藤嘉浩：工業材料, **52**, 12-13 (2004)
3) 伊藤嘉浩：表面科学, **25**, 16-22 (2004)
4) 伊藤嘉浩，金野智浩，宮本寛治：バイオインダストリー, **21**, 5-11 (2004)
5) 伊藤嘉浩, 野川誠之, 金野智浩, 牧野　弘, 蓮田寛和, 宮本寛治, 池淵研二：再生医療学会誌, **3**, 55-61 (2004)
6) 伊藤嘉浩：*Organ Biology*, **12**, 47-55 (2005)
7) 伊藤嘉浩：未来材料, **5**, 46-47 (2005)
8) 伊藤嘉浩：「図解高分子新素材のすべて」，国武豊喜監修, 工業調査会, pp. 94-97 (2005)
9) 伊藤嘉浩：化学, **62**, 38-41 (2007)
10) 伊藤嘉浩：「高分子材料・技術総覧」，高分子材料・技術総覧編集委員会, 産業技術サービスセンター, pp.615-622 (2004)
11) 野川誠之, 伊藤嘉浩：遺伝子医学 Mook, **1**, 88-93 (2004)
12) 北嶋　隆, 伊藤嘉浩：再生医療学会誌, **4**, 53-61 (2005)
13) 伊藤嘉浩：「再生医療」，田畑泰彦, 赤池敏宏編集, コロナ社, pp.221-235 (2006)
14) Ito Y : *Soft Matter*, in press (2007)
15) Ito Y, Hasuda H, Kitajima T, Kiyono T : *J. Biosci. Bioeng.*, **102**, 467-469 (2006)
16) Miyamoto K, Hayashi K, Suzuki T, Ichihara S, Yamada T, Kano Y, Yamabe T, Ito Y : *Stem Cells*, **22**, 433-440 (2004)
17) Ito Y, Kawamorita M, Yamabe T, Kiyono T, Miyamoto K : *J. Biosci. Bioeng.*, **103**, 113-121 (2007)
18) Ito Y, Hasuda H, Terada H, Kitajima T : *J. Biomed. Mater. Res.*, **74**, 659-665 (2005)
19) Ito Y, Hasuda H, Yamauchi T, Komatsu N, Ikebuchi K : *Biomaterials*, **25**, 2293-2298 (2004)
20) Makino H, Hasuda H, Ito Y : *J. Biosci. Bioeng.*, **98**, 374-379 (2004)

(Received 22 June 2007;
Accepted 10 July 2007)

著者略歴

伊藤　嘉浩（いとう　よしひろ）

1981年3月　京都大学工学部高分子化学科卒業
1986年3月　同大学大学院工学研究科研究指導認定退学
1987年1月　同大学工学博士
1988年4月　同大学　助手
1996年2月　同大学大学院　助教授
1997年4月　奈良先端科学技術大学院大学　助教授
1999年4月　徳島大学　教授
2002年4月　神奈川科学技術アカデミー　プロジェクトリーダー
2004年5月　理化学研究所　主任研究員

幹細胞培養のための ナノ界面創成バイオリアクター

伊藤嘉浩（いとうよしひろ）
（独）理化学研究所伊藤ナノ医工学研究室

再生医療の話題は，科学を超えて事欠かない．2004年のアメリカ大統領選では，胚性幹（ES）細胞の研究が争点の一つになり，結局，ヒトES細胞研究に消極的なブッシュ大統領が勝利した．しかしその後，シュワルツェネッガー知事のカリフォルニア州では，住民投票による賛成多数の支持を受け，ヒトES細胞研究を中心とした再生医療の基礎研究に対し，今後10年間で州予算から約30億ドルを出資することになった．また，2005年末から2006年はじめにかけては，韓国でのクローン化ヒトES細胞のねつ造問題が世界中の注目の的となった．

「夢の医療」として再生医療が注目を集めるようになった経緯を図1に示す．もともと，病気で機能障害や機能不全に陥った生体組織・臓器の治療のために，近代的な人工臓器や臓器移植が発展してきた．しかし，人工臓器の高性能化には現在のところ限界があり，臓器移植ではドナーの不足が深刻である．日本で脳死移植が可能となった1997年の臓器移植法の施行以来，現在までの移植件数は50件ほどにとどまっている．そのようななか，1980年代後半からハイブリッド人工臓器の先駆けとなった培養皮膚の考えを発展させた「生体組織工学（tissue engineering）」という概念が生まれた．これは，生分解性マトリックスを足場にして生体内外で組織再生を行わせようとするものであった．そして1990年代後半になると，クローン技術の発明（クローン羊の誕生）と，ヒトES細胞の樹立という二つの大きな進展により「再生医療」という，幹細胞を積極的に利用して生体機能の再生を図る医療が考えられるようになった[1]．

再生医療のための幹細胞

再生医療への期待が膨らんだ背景には，ヒトES細胞の樹立以外に，成人体内でも多くの幹細胞が存在することが明らかになってきたからである．幹細胞とは，さまざまな細胞へ

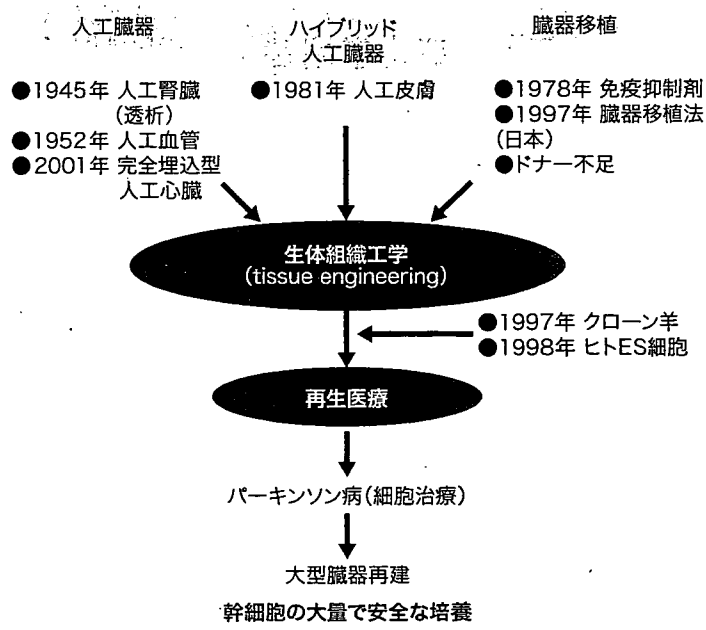

図1　再生医療研究への流れ

伊藤嘉浩（いとう よしひろ）
＜所属＞（独）理化学研究所主任研究員（伊藤ナノ医工学研究室），＜出身大学＞京都大学（1981年卒業），＜研究テーマ＞再生医療工学，コンビナトリアルバイオエンジニアリング，ソフトナノテクノロジー，＜趣味＞そぞろ歩き